Earth, Planets and Space

EXPRESS LETTER

Open Access

Kusatsu-Shirane volcano eruption on January 23, 2018, observed using JMA operational weather radars

Eiichi Sato*

Abstract

A phreatic eruption suddenly occurred at Motoshirane (Kusatsu-Shirane volcano, Japan) at 10:02 JST on January 23, 2018. A member of the Japan Self-Defense Force was killed by volcanic blocks during training in Motoshirane, and 11 people were injured by volcanic blocks or fragments of broken glass. According to a field survey, ash fall was confirmed in Minakami, about 40 km east-northeast from Motoshirane. Although the eruption was not captured by a distant camera, the eruption plume/cloud was captured by three of the Japan Meteorological Agency's operational weather radars. These radars observed the echo propagated to the northeast in the lower troposphere, and to the east in the middle troposphere. This is generally consistent with the observed ash fall distribution. Using the modified probabilistic estimation method, the maximum plume height was estimated to be about 5580 ± 506 m (1σ) above sea level. Estimates of the erupted mass based on the range of plume heights from radar observations and the duration of volcanic tremor during the eruption (about 8 min) do not match that obtained from a field survey ($3.0–5.0 \times 10^7$ kg). This discrepancy confirms that estimates of erupted mass based on plume heights must account for eruption style parametrically, which can only be constrained by case studies of varied eruption styles.

Keywords: Weather radar, Remote sensing, Volcanic plume, Eruption cloud, Kusatsu-shirane volcano

Introduction

Weather radar is usually used to observe rain, but it is also a useful tool for detecting volcanic eruptions. In fact, many volcanic eruptions have been captured by weather radar (e.g., Sawada 2003; Marzano et al. 2013). However, it is difficult to estimate plume heights by using remote sensing instruments that transmit and receive radio waves, such as weather radar, because of error resulting from the influence of the beam width. To reduce this error, Sato et al. (2018) developed a probabilistic estimation (PE) method and applied it to the 2016 eruption of Mt. Aso. They derived the total amount of ejecta from the radar data and obtained a value consistent with a field survey. Nonetheless, it is important to confirm the validity of their method for other cases and eruption styles, particularly phreatic eruptions. For magmatic eruptions, several empirical formulas have been proposed to estimate the amount of ejecta using the plume height (e.g., Costa et al. 2016), but it is not clear whether they are also valid for phreatic eruptions. Therefore, one of the objectives of this paper is to test the validity of the empirical formulas for phreatic eruptions.

Kusatsu-Shirane volcano

Kusatsu-Shirane volcano, a complex volcano in the northwestern tip of Gunma prefecture, central Honshu, Japan, comprises three independent pyroclastic cone groups aligned from north to south: Shirane, Ainomine, and Motoshirane (Fig. 1). Magmatic eruptions occurred repeatedly at Motoshirane until 1500 years ago (e.g., Nigorikawa et al. 2016; Ishizaki et al. 2020), whereas recent

*Correspondence: esato@mri-jma.go.jp
Meterological Research Institute, 1-1 Nagamine, Ibaraki 305-0052 Tsukuba, Japan

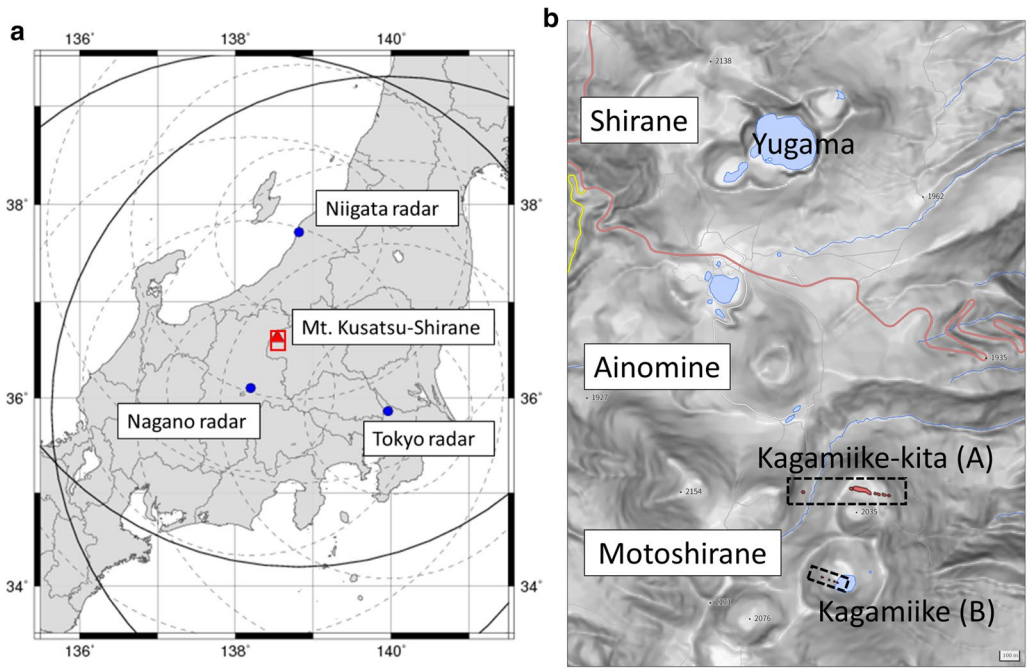

Fig. 1 **a** Location map of three JMA weather radars (blue dots) around Mt. Kusatsu-Shirane (red triangle). Dashed concentric circles show 100, 200, and 300 km from each radar site, and solid circles show the maximum range of the radars (400 km). **b** Detailed map around Mt, Kusatsu-Shirane. This area corresponds to the red rectangle in **a**. Two dashed rectangles show the crater rows [Kagamiike-kita (**A**) and Kagamiike (**B**)] of the 2018 eruption. This figure was created based on the map created on the Geospatial Information Authority of Japan website (https://maps.gsi.go.jp/vector/)

eruptive activity is characterized by phreatic eruptions at Shirane, with most eruptions occurring around Yugama crater (e.g., Terada 2018). Therefore, many geochemical studies have been conducted on Kusatsu-Shirane volcano, especially on the hydrothermal system around Shirane (e.g., Ossaka et al. 1980, 1997; Sano et al. 1994; Ohba et al. 1994, 2000, 2008, 2019). Nurhassan et al. (2006), Matsunaga et al. (2020) and Tseng et al. (2020) revealed the three-dimensional structure of the Kusatsu-Shirane hydrothermal system using the magnetotelluric (MT) or audio-frequency magnetotelluric method. In particular, Matsunaga et al. (2020) reported the existence of an extensive low resistivity layer at depths of 1–3.5 km beneath the summit of Motoshirane using MT data collected in 2015 and 2016. This layer was interpreted as a hydrothermal fluid reservoir.

In 2018, the first historical eruption at Motoshirane occurred.

Phreatic eruption on January 23, 2018

The Coordinating Committee for Prediction of Volcanic Eruptions (CCPVE 2018) stated that an eruption occurred at Motoshirane around 10:02 JST on January 23, 2018. CCPVE also estimated that the eruption occurred along an east–west row of new craters 500 m long on the north side of the crater of the Kagamiike-kita pyroclastic cone (crater raw A). After that, another crater row (crater raw B) was found near Kagamiike (Japan Meteorological Agency (JMA) 2018). This eruption ejected large volcanic bombs over 1 km from the crater (CCPVE 2018). The eruption was accompanied by about 8 min of volcanic tremor with large amplitude that began at 09:59JST (CCPVE 2018).

One Japan Self-Defence Force (SDF) member who was training at Motoshirane was killed during the eruption, and seven other members were injured nearby (Fire and Disaster Management Agency 2018). The eruption caused the ropeway at Kusatsu International Ski Resort to stop, stranding 81 people in the gondolas, four of whom were injured by a windowpane that was broken by the impact of volcanic bombs. According to a field survey conducted by the Joint Research Team for Ash Fall in Kusatsu-Shirane 2018 eruption (2018b), ash fall was also confirmed in Minakami, a town about 40 km east-northeast of Motoshirane.

The total erupted mass was estimated to be 3.0–5.0×10^7 kg by the Joint Research Team for Ash Fall in Kusatsu-Shirane 2018 eruption (2018a). As a result of the investigation of the ejecta, the National Institute of Advanced Industrial Science and Technology and the

National Research Institute for Earth Science and Disaster Prevention (2018) concluded that the eruption had likely been a phreatic eruption. Yaguchi et al. (2019) also analyzed the volcanic ash of the 2018 eruption of Motoshirane, and showed that the explosion had occurred at a depth reaching the basement rocks (i.e., more than 100 m deep) and in a relatively gas phase-rich condition as compared with the 1982 eruption of Shirane.

Using the volcanic tremor data, Yamada et al. (2021) revealed that the 2018 eruption had been triggered by hydrothermal fluid injection through a different pathway from that of unrest activities at Yugama since 2014. Himematsu et al. (2020) analyzed the crustal deformation associated with the eruption using satellite synthetic aperture radar data. The dislocation plane inferred by them can be considered as a degassing pathway to the surface associated with the eruption.

A JMA camera at Ainomine, located 800 m from the crater raw A, did not observe the eruption, but three JMA weather radars (Nagano, Niigata, and Tokyo; Fig. 1) captured the echo of the eruption plume/cloud. The radar echo was observed to move northeast in the lower troposphere, and east in the middle troposphere (Fig. 2). These multi-station radar observations are consistent with the ash fall distribution reported by the Joint Research Team (2018a; b).

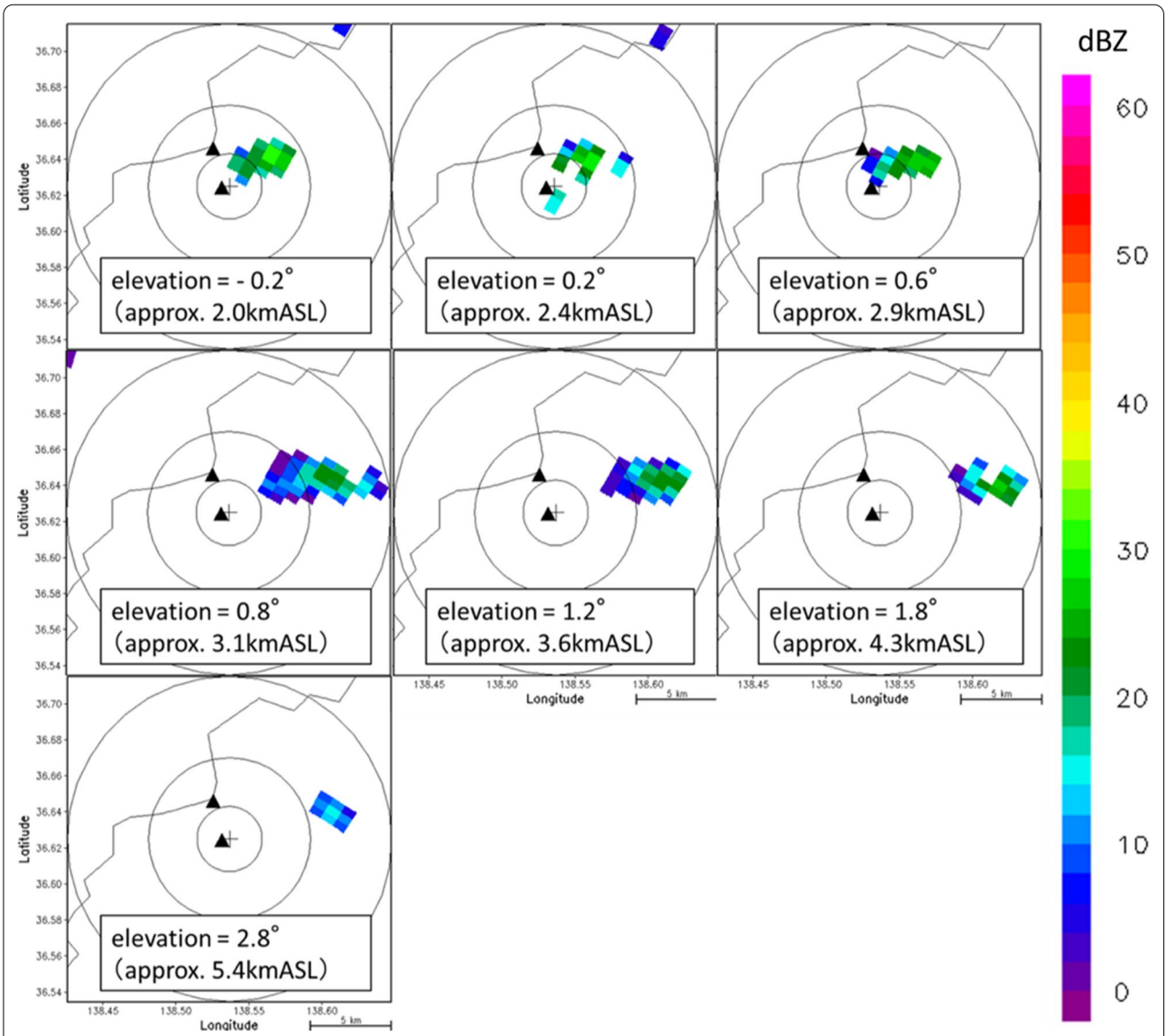

Fig. 2 Reflectivity images observed by Nagano radar between 10:05 and 10:10 JST on January 23, 2018. Black triangles show summits of Motoshirane and Shirane. Concentric circles show 2, 5, and 10 km from the v (+). Elevations in each panel show elevation angles of Nagano radar

Methodology

Modified probabilistic estimation method

In order to investigate the height of the eruption plume from its radar echo, the author developed a modified probabilistic estimation (MPE) method, an improved version of the PE method (Sato et al. 2018).

The path of radio waves in the spherically stratified atmosphere is expressed as (e.g., Hartree et al. 1946; Battan 1973):

$$\frac{d^2h}{ds^2} - \left(\frac{2}{R+h} + \frac{1}{n}\frac{dn}{dh}\right)\left(\frac{dh}{ds}\right)^2 - \left(\frac{R+h}{R}\right)^2\left(\frac{1}{R+h} + \frac{1}{n}\frac{dn}{dh}\right) = 0, \tag{1}$$

where h is the altitude above the surface of the Earth, s is the horizontal distance, R is the radius of the Earth, and n is the refractive index of the atmosphere.

Assuming $(dh/ds)^2 \ll 1$, $n \approx 1$ and $h \ll R$, Eq. (1) is simplified to:

$$\frac{d^2h}{ds^2} = \frac{1}{R} + \frac{dn}{dh}. \tag{2}$$

If the elevation angle θ_e of the beam path is small, it can be assumed that $dh/ds \approx \theta_e$, and Eq. (2) becomes:

$$\frac{d\theta_\mathrm{e}}{ds} = \frac{1}{R} + \frac{dn}{dh} = \frac{1}{k_\mathrm{e}R}, \tag{3}$$

where k_e is the equivalent radius ratio (e.g., Doviak and Zrnic 1993; Sato et al. 2018).

Whereas the PE method assumes the 4/3 R equivalent earth radius model, the MPE method incorporates the ellipticity of the Earth by using Euler's (1767) radius of curvature:

$$R_\varphi^\alpha = \frac{M_\varphi N_\varphi}{N_\varphi \cos^2\alpha + M_\varphi \sin^2\alpha}. \tag{4}$$

Here, M_φ is the radius of curvature of the meridian at latitude φ, N_φ is the radius of curvature of the prime vertical, and α is the azimuth of the target relative to the radar. Using R_φ^α obtained for each radar, Eq. (3) becomes:

$$\frac{1}{k_\mathrm{e}R} = \frac{1}{R_\varphi^\alpha} + \frac{dn}{dh}. \tag{5}$$

We obtained dn/dh from the mean field of the lower atmosphere (< 5 km altitude) between the radar and the target by using the initial value of the JMA Mesoscale Model (MSM) at 0:00 UTC on January 23, 2018 as the atmospheric field. Since the MSM does not explicitly predict the refractive index of the atmosphere, it was calculated as:

$$N = (n-1)\times 10^6 = 7.76\times 10^{-5}\frac{p}{T} + 3.75\times 10^5\frac{e}{T^2}, \tag{6}$$

where N is refractivity, p is atmospheric pressure, T is air temperature, and e is vapor pressure (e.g., Bean and Dutton 1968). Saturated water vapor pressure e_s was approximated by using the expression used by the World Meteorological Organization (e.g., Mizuno 2000):

$$e_s = \exp[19.482 - 4303.4/(T_\mathrm{c} + 243.5)], \tag{7}$$

where T_c is the atmospheric temperature in degrees Celsius. In the MPE method, these formulas are used to obtain the equivalent earth radius ratio for each radar.

Next, we derived the probabilistic estimation equations used in the MPE method. In the PE method, the radar beam height that captures the plume is calculated by:

$$h = (k_eR + h_0)\left[\frac{\cos\theta_\mathrm{e}}{\cos\{\theta_\mathrm{e} + s/(k_\mathrm{e}R)\}} - 1\right] + h_0, \tag{8}$$

where h_0 is the antenna height. The JMA weather radars perform 28 scans per 10 min over a range of elevation angles from about 0 to 25 degrees. Furthermore, for the low elevation angles used in this study (about 0–5°), most of the angles are scanned twice, and as a result, the time resolution is about 5 min. Whether the target echo was caused by volcanic plumes or not is judged from the continuity between elevation angles.

One of the improvements from the PE method is a geoid correction. Whereas the PE method does not consider the geoid height for height estimations, the MPE method includes a geoid correction. Specifically, because the antenna height is usually given relative to the geoid, the geoid height at the location of the radar $h_{G,\mathrm{radar}}$ is added to convert the antenna height to an altitude relative to the Earth ellipsoid. Then, after deriving the altitude of the target, the geoid height at the location of the target $h_{G,\mathrm{target}}$ is subtracted to convert the target height to an altitude relative to the geoid. For the geoid height, GSIGEO2011 by the Geospatial Information Authority of Japan (2016) was used. By this correction, Eq. (8) becomes:

$$h = \left(k_\mathrm{e}R + h_0 + h_{G,\mathrm{radar}}\right)\left[\frac{\cos\theta_\mathrm{e}}{\cos\{\theta_\mathrm{e} + s/(k_\mathrm{e}R)\}} - 1\right] + h_0 + h_{G,\mathrm{radar}} - h_{G,\mathrm{target}}. \tag{9}$$

The obtained heights are treated as altitudes above sea level (m ASL).

The probability density function of the heights obtained by each radar is calculated as:

$$f_i(h_j) = \frac{1}{\sqrt{2\pi}\sigma_i}\exp\left\{-\frac{(h_j-\mu_i)^2}{2\sigma_i^2}\right\}. \quad (10)$$

Here, $h_j(=j\Delta h)$ is the discretized height above sea level ($j=0,1,2\ldots,\infty$), and μ_i and σ_i are the median height and standard deviation of the ith radar, respectively. In addition, we assume that $\mu_i = H_c$, $\sigma_i = \beta(H_u - H_l)/2$ and $\beta = 1$. H_c is the altitude at the center of the beam, H_u is the altitude at the top of the beam, and H_l is the altitude at the bottom of the beam. Finally, the composite probability density combining all radars is obtained as:

$$f_{\text{composite}}(h_j) = \frac{\prod_{i=1}^{n} f_i(h_j)}{\sum_{j=0}^{\infty}\{\prod_{i=1}^{n} f_i(h_j)\}\Delta h}. \quad (11)$$

Erupted mass estimation methods

One of the author's goals is to quickly estimate the scale of the eruption, that is, the erupted mass, using the eruption plume height estimated by weather radars. We used four empirical methods in Costa et al. (2016) to estimate the total mass of ejecta by the 2018 Kusatsu-Shirane eruption. For simplicity, each model is reproduced as closely as possible from the literature, and the variables in this section are independent of those used in the preceding section. We briefly describe each method and the references therein which provide more detailed information.

The method of Carazzo et al. (2014; hereafter 'C14') estimates the mass eruption rate $\dot{M}$[kg/s] of weak mid-latitude plume es:

$$\ln(\dot{M}) = \ln(b_1 H^{n_1}) + cWH, \quad (12)$$

where H is the maximum observed plume height [km], $W = 83.66$m/s is the wind velocity at the tropopause height, and $n_1 = 4.06$, $b_1 = 63.22$ and $c = 0.0025$ are fitting parameters.

The method of Degruyter and Bonadonna (2012; hereafter 'DB12') calculates $\dot{M}$ as:

$$\dot{M} = \pi\frac{\rho_{a0}}{g'}\left(\frac{2^{5/2}\alpha^2\overline{N}^3}{z_l^4}H^4 + \frac{\beta^2\overline{N}^2\overline{v}}{6}H^3\right), \quad (13)$$

where $\rho_{a0} = 1.105\text{kg/m}^3$ is the density of the atmosphere, $g' = 41.289\text{m/s}^2$ is the reduced gravity at the plume source, $\alpha = 0.1$ is the radial entrainment coefficient, $\overline{N} = 0.0134\text{s}^{-1}$ is the average buoyancy, $z_l = 2.8$ is the maximum non-dimensional height of Morton et al. (1956), $\beta = 0.5$ is the wind entrainment coefficient, and $\overline{v} = 31.3935$m/s is the average wind velocity over the plume height.

Mastin et al. (2009; hereinafter 'M09') estimated $\dot{M}$ as:

$$\dot{M} = \rho_m(H/2)^{4.15}, \quad (14)$$

where $\rho_m = 2500\text{kg/m}^3$ is the density of magma. M09 estimated the volumetric flow rate (dense-rock equivalent) $\dot{V}\left[\text{m}^3/s\right]$ at first, and converted it to $\dot{M}$ with this magma density.

Finally, the method of Woodhouse et al. (2013, 2016; hereafter 'W16') uses:

$$\dot{M} = 0.35\alpha^2 f(W_s)^4\frac{\rho_{a0}}{g'}N^3H^4, \quad (15)$$

$$f(W_s) = \frac{1 + 1.4266W_s + 0.3527W_s^2}{1 + 1.373W_s}, \quad (16)$$

$$W_s = 1.44\dot{\gamma}/N, \quad (17)$$

and,

$$g' = g\left[\frac{(C_v n_0 + C_s(1-n_0))\theta_0 - C_a\theta_{a0}}{C_a\theta_{a0}}\right]. \quad (18)$$

Here, W_s is a dimensionless wind strength, $\alpha = 0.09$, $\rho_{a0} = 1.104\text{kg/m}^3$, $\theta_0 = 1273$K and $\theta_{a0} = 268.8$K are the source temperature and the atmospheric temperature, respectively, $N = 0.014\text{s}^{-1}$, $\dot{\gamma} = 0.007\text{s}^{-1}$ is the shear rate of the atmospheric wind, $n_0 = 0.03$ is the mass fraction of gas at the vent, $C_v = 1810\text{J}/(\text{kg K})$, $C_s = 1100\text{J}/(\text{kg K})$, and $C_a = 1000\text{J}/(\text{kg K})$ are the specific heat capacity at constant pressure of water vapor, solid pyroclasts, and dry air, respectively.

Results

Table 1 shows the range of eruption altitudes obtained by each radar and the final combined results. Using Eq. (5), k_e is calculated from R_φ^α and dn/dh derived for each radar. The ranges of eruption altitude were calculated from Eq. (9) using k_e. The MPE method assumes a probability

Table 1 Plume heights estimated for each radar, and composite plume height

Radar site	R_φ^α [m]	$\frac{dn}{dh}$	k_e	Median plume height [m ASL]	Standard deviation [m]
Nagano	6,365,417	− 2.571E−08	1.195	5692	632
Niigata	6,359,764	− 2.655E−08	1.201	5133	1091
Tokyo	6,375,958	− 2.829E−08	1.221	5776	1330
Composite	–	–	–	5580	506

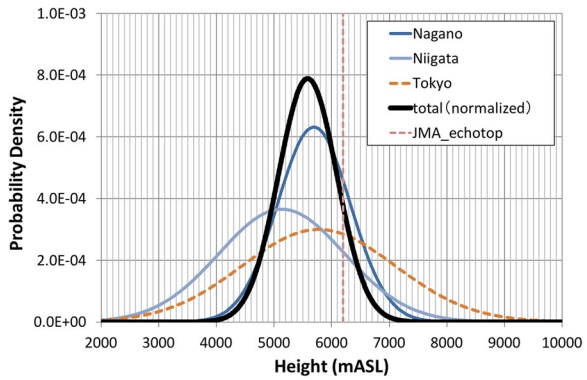

Fig. 3 Probability densities of plume height estimated for each radar (thin colored curves) and composite plume height (thick black line). The pink, dashed vertical line at 6200 m ASL indicates radar echo height determined by JMA

Table 2 Erupted masses estimated using four empirical methods and from a field survey

Method	Erupted mass [kg]
Carazzo et al. (2014)	5.1×10^6–2.0×10^7
Degruyter and Bonadonna (2012)	2.7×10^8–6.5×10^8
Mastin et al. (2009)	6.7×10^6–2.2×10^7
Woodhouse et al. (2013, 2016)	1.2×10^7–3.9×10^7
Field survey	3.0×10^7–5.0×10^7

density function with a normal distribution (Eq. 10), and derives the center of the beam (median value) and the standard deviation from it. The maximum plume height of the 2018 Kusatsu-Shirane eruption obtained by using Eq. (11) results in a composite estimate of 5580 ± 506 m ASL (Fig. 3; Table 1). Because there is no large variation among the results obtained from each radar, we consider that anomalous propagation did not occur.

Table 2 shows that estimates of the erupted mass by each empirical method, based on the range of the composite plume height in Table 1. All methods except DB12 underestimate the total erupted mass compared to the field survey.

Discussion

One of the reasons for the underestimation in most models (Table 2) seems to be related to the application of the empirical formulas created from magmatic eruptive events and less applicable to phreatic activity. The same tendency was confirmed when we applied the empirical formulas to the 2014 Mt. Ontake eruption, which is also a phreatic eruption. In this calculation, the maximum eruption height is assumed to be 8.0 km ASL (5.3 km above crater) obtained by a photograph (Sato et al. 2016). It is also assumed that most of the ejecta erupted within about 25 min (Maeno et al. 2016). In other words, the duration of the 2014 Mt. Ontake eruption is assumed to be 25 min.

Only the DB12 method overestimated the erupted mass (Table 2), possibly because it overemphasizes the effect of entrainment by wind (i.e., the second term on the right-hand side of Eq. (13). Suzuki and Koyaguchi (2015) estimated the entrainment coefficient β to be 0.1–0.3 from the calculation results of a 3-D model, therefore, there is a possibility that only the coefficient was a problem.

Nonetheless, none of the methods provided a satisfactory estimate of the erupted mass. Each method requires minor modifications according to the eruption style, in this case, a phreatic eruption. Therefore, it is necessary to accumulate far more eruption case studies and clarify the detailed relationships between the various physical quantities and the total erupted mass for the range of phreatic eruptions.

Summary and conclusion

The eruptive plume/cloud echo associated with the Kusatsu-Shirane eruption on January 23, 2018, was captured by three operational JMA weather radars. The echo moved northeast in the lower troposphere, and east in the middle troposphere. These radar observations were consistent with the observed ash deposition patterns. Using the MPE method, the plume height was estimated to be about 5580 ± 506 m ASL (1σ). The amount of the ejecta estimated from this result and the duration of volcanic tremor associated with the eruption (about 8 min) did not match the mass estimated by the field survey (3.0–5.0×10^7 kg). More specifically, the estimates of the erupted mass by the three methods (C14, M09 and W16) were less than half of the field survey, while only DB12 overestimated it. One of the reasons seems to be that these empirical formulas are not applicable to phreatic eruptions without change. This implies that estimates of the total erupted mass based on plume height must account for eruption style by selecting reasonable model parameter values, which can only be constrained by further case studies incorporating varied eruption styles.

Abbreviations

JST: Japan Standard Time; MT: Magnetotelluric; CCPVE: Coordinating Committee for Prediction of Volcanic Eruptions; JMA: Japan Meteorological Agency.

Acknowledgements

I would like to express my gratitude to three anonymous reviewers and Dr. Arthur Jolly, the handling editor, for their useful comments and suggestions. JMA operational weather radar data were provided by the Observation Department of JMA Headquarters. I also thank Dr. Toshiki Shimbori of the Meteorological Research Institute (MRI) for teaching me how to read GPV data, and Dr. Muga Yaguchi of MRI for providing me with valuable information on geochemical features of the 2018 Kusatsu-Shirane volcano eruption.

Authors' contributions
ES gathered and analyzed the radar data, and performed the probabilistic estimation. The author read and approved the final manuscript.

Authors' information
ES is a senior researcher at the Meteorological Research Institute.

Funding
Not applicable.

Availability of data and materials
The original radar data were provided by the Observation Department of JMA, and the author does not have the rights to share them. The processed data that support the findings of this study are available from the author upon reasonable request.

Declarations

Ethics approval and consent to participate
Not applicable.

Consent for publication
Not applicable.

Competing interests
No competing interests.

Received: 31 December 2020 Accepted: 24 May 2021
Published online: 31 May 2021

References

Battan LJ (1973) Radar observation of the atmosphere. University of Chicago Press, Chicago

Bean BR, Dutton EJ (1968) Radio meteorology. Dover Publications, New York

Carazzo G, Girault F, Aubry T, Bouquerel H, Kaminski E (2014) Laboratory experiments of forced plumes in a density-stratified crossflow and implications for volcanic plumes. Geophys Res Lett 41:8759–8766. https://doi.org/10.1002/2014GL061887

Coordinating Committee for Prediction of Volcanic Eruptions (2018) Official opinion on Kusatsu-Shirane Volcano activity. https://www.jma.go.jp/jma/press/1801/26a/yochiren180126-1.pdf. Accessed 25 Jan 2021. **(In Japanese)**

Costa A, Suzuki YJ, Cerminara M, Devenish BJ, Esposti Ongaro T, Herzog M, Van Eaton AR, Denby LC, Bursik M, de MichieliVitturi M, Engwell S, Neri A, Barsotti S, Folch A, Macedonio G, Girault F, Carazzo G, Tait S, Kaminski E, Mastin LG, Woodhouse MJ, Phillips JC, Hogg AJ, Degruyter W, Bonadonna C (2016) Results of the eruptive column model intercomparison study. J Volcanol Geotherm Res 326:2–25. https://doi.org/10.1016/j.jvolgeores.2016.01.017

Degruyter W, Bonadonna C (2012) Improving on mass flow rate estimates of volcanic eruptions. Geophys Res Lett 39:L16308. https://doi.org/10.1029/2012GL052566

Doviak RJ, Zrnic DS (1993) Doppler radar and weather observations, 2nd edn. Academic Press, San Diego

Euler L (1767) Recherches sur la courbure des surfaces. Histoire de l'Académie royale des sciences et des belles lettres de Berlin 16:119–143

Fire and Disaster Management Agency (2018) Damage caused by volcanic activity of Motoshirane and the responses of fire departments (9th report). https://www.fdma.go.jp/disaster/info/assets/post872.pdf Accessed 21 Jan 2021. **(In Japanese)**

Geospatial Information Authority of Japan (2016) GSIGEO2011(Ver.2.1). https://www.gsi.go.jp/buturisokuchi/grageo_geoidseika.html. Accessed 31 Dec 2020. **(In Japanese)**

Hartree DR, Michel JGL, Nicholson P (1946) Practical methods for the solution of the equations of tropospheric refraction. In: Meteorological factors in radio wave propagation. Physical Society, London, pp. 127–168

Himematsu Y, Ozawa T, Aoki Y (2020) Coeruptive and posteruptive crustal deformation associated with the 2018 Kusatsu-Shirane phreatic eruption based on PALSAR-2 time series analysis. Earth Planets Space 72:116. https://doi.org/10.1186/s40623-020-01247-6

Ishizaki Y, Nigorikawa A, Kametani N, Yoshimoto M, Terada A (2020) Geology and eruption history of the Motoshirane Pyroclastic Cone Group, Kusatsu-Shirane Volcano, central Japan. J Geol Soc Japan 126:473–491. https://doi.org/10.5575/geosoc.2020.0022 (**In Japanese with English abstract**)

Japan Meteorological Agency (2018) Volcanic Activity of Kusatsu-Shiranesan Volcano (October 2017–February 2018), Rep. Coordinating Committee for Prediction of Volcanic Eruptions No. 129, Japan Meteorological Agency, Tokyo. https://www.data.jma.go.jp/svd/vois/data/tokyo/STOCK/kaisetsu/CCPVE/Report/129/kaiho_129_07.pdf. Accessed 21 Feb 2021. **(In Japanese)**

Joint Research Team for Ash Fall in Kusatsu-Shirane 2018 eruption (2018a) Ash fall distribution of Jan. 23, 2018 eruption in Kusatsu-Shirane Volcano. Materials for 140th meeting of Coordinating Committee for the Prediction of Volcanic Eruption. https://www.data.jma.go.jp/svd/vois/data/tokyo/STOCK/kaisetsu/CCPVE/shiryo/140/140_01-1-1.pdf. Accessed 21 Feb 2021. **(In Japanese)**

Joint Research Team for Ash Fall in Kusatsu-Shirane 2018 eruption (2018b) Ash fall distribution of Jan. 23, 2018 eruption in Kusatsu-Shirane Volcano. Rep. Coordinating Committee for Prediction of Volcanic Eruptions No. 129, Japan Meteorological Agency, Tokyo. https://www.data.jma.go.jp/svd/vois/data/tokyo/STOCK/kaisetsu/CCPVE/Report/129/kaiho_129_10.pdf. Accessed 25 January 2021. **(In Japanese)**

Maeno F, Nakada S, Oikawa T, Yoshimoto M, Komori J, Ishizuka Y, Takeshita Y, Shimano T, Kaneko T, Nagai M (2016) Reconstruction of a phreatic eruption on 27 September 2014 at Ontake volcano, central Japan, based on proximal pyroclastic density current and fallout deposits. Earth Planets Space 68:82. https://doi.org/10.1186/s40623-016-0449-6

Marzano FS, Picciotti E, Montopoli M, Vulpiani G (2013) Inside volcanic clouds: remote sensing of ash plumes using microwave weather radars. Bull Am Meteorol Soc 94:1567–1586. https://doi.org/10.1175/BAMS-D-11-00160.1

Mastin LG, Guffanti M, Servanckx R, Webley P, Barsotti S, Dean K, Durant A, Ewert JW, Neri A, Rose WI, Schneider D, Siebert L, Stunder B, Swanson G, Tupper A, Volentik A, Waythomas CF (2009) A multidisciplinary effort to assign realistic source parameters to models of volcanic ash-cloud transport and dispersion during eruptions. J Volcanol Geotherm Res 186:10–21. https://doi.org/10.1016/j.jvolgeores.2009.01.008

Matsunaga Y, Kanda W, Takakura S, Koyama T, Saito Z, Seki K, Suzuki A, Kishita T, Kinoshita Y, Ogawa Y (2020) Magmatic hydrothermal system inferred from the resistivity structure of Kusatsu-Shirane Volcano. J Volcanol Geotherm Res 390:106742. https://doi.org/10.1016/j.jvolgeores.2019.106742

Mizuno H (2000) Cloud and rain meteorology. Asakura Publishing, Tokyo **(In Japanese)**

Morton BR, Tayler GT, Turner JS (1956) Turbulent gravitational convection from maintained and instantaneous sources. Proc R Soc Lond A 234:1–23. https://doi.org/10.1098/rspa.1956.0011

National Institute of Advanced Industrial Science and Technology and National Research Institute for Earth Science and Disaster Resilience (2018) Characteristics of the constituent particles of the Kusatsu-Shirane volcanic product on January 23, 2018. https://www.gsj.jp/hazards/volcano/kazan-bukai/yochiren/kusatsushirane_20180124_1.pdf. Accessed 25 Jan 2021. **(In Japanese)**

Nigorikawa A, Ishizaki Y, Kametani N, Yoshimoto M, Terada A, Ueki K, Nakamura K (2016) Holocene eruption history of the Motoshirane Pyroclastic Cone Group, Kusatsu-Shirane Volcano. Abstracts of Japan Geoscience Union Meeting 2016 SVC48–11. https://confit.atlas.jp/guide/event/jpgu2016/subject/SVC48-11/detail. Accessed 7 May 2021

Nurhasan OY, Ujihara N, Tank SB, Honkura Y, Onizawa S, Mori T, Makino M (2006) Two electrical conductors beneath Kusatsu-Shirane volcano, Japan, imaged by audiomagnetotellurics, and their implications for the hydrothermal system. Earth Planets Space 58:1053–1059. https://doi.org/10.1186/BF03352610

Ohba T, Hirabayashi J, Nogami K (1994) Water, heat and chloride budgets of the crater lake, Yugama at Kusatsu-Shirane volcano, Japan. Geochem J 28:217–231. https://doi.org/10.2343/geochemj.28.217
Ohba T, Hirabayashi J, Nogami K (2000) D/H and $^{18}O/^{16}O$ ratios of water in the crater lake at Kusatsu-Shirane volcano, Japan. J Volcanol Geotherm Res 97:329–346. https://doi.org/10.1016/S0377-0273(99)00169-9
Ohba T, Hirabayashi J, Nogami K (2008) Temporal changes in the chemistry of lake water within Yugama Crater, Kusatsu-Shirane Volcano, Japan: implications for the evolution of the magmatic hydrothermal system. J Volcanol Geotherm Res 178:131–144. https://doi.org/10.1016/j.jvolgeores.2008.06.015
Ohba T, Yaguchi M, Nishino K, Numanami N, Tsunogai U, Ito M, Shingubara R (2019) Time variation in the chemical and isotopic composition of fumarolic gasses at Kusatsu-Shirane volcano, Japan. Front Earth Sci 7:249. https://doi.org/10.3389/feart.2019.00249
Ossaka J, Ozawa T, Nomura T, Ossaka T, Hirabayashi J, Takaesu A, Hayashi T (1980) Variation of chemical compositions in volcanic gases and waters at Kusatsu-Shirane volcano and its activity in 1976. Bull Volcanol 43:207–216. https://doi.org/10.1007/BF02597622
Ossaka J, Ossaka T, Hirabayashi J, Oi T, Ohba T, Nogami K, Kikawada Y, Yamano M, Yui M, Fukuhara H (1997) Volcanic activity of Kusatsu-Shirane volcano, Gunma, and secular change in water quality of crater lake Yugama. Chikyukagaku (geochem) 31:119–128. https://doi.org/10.14934/chikyukagaku.31.119
Sano Y, Hirabayashi J, Oba T, Gamo T (1994) Carbon and helium isotopic ratios at Kusatsu-Shirane Volcano, Japan. Appl Geochem 9:371–377. https://doi.org/10.1016/0883-2927(94)90059-0
Sato E, Fukui K, Shimbori T (2018) Aso volcano eruption on October 8, 2016, observed by weather radars. Earth Planets Space 70:105. https://doi.org/10.1186/s40623-018-0879-4
Sato E, Shimbori T, Fukui K, Ishii K, Takagi A (2016) The eruption cloud echo from Mt. Ontake on September 27, 2014 observed by weather radar network. Rep. Coordinating Committee for Prediction of Volcanic Eruptions No. 119, Japan Meteorological Agency, Tokyo. https://www.data.jma.go.jp/svd/vois/data/tokyo/STOCK/kaisetsu/CCPVE/Report/119/kaiho_119_11.pdf. Accessed 21 Feb 2021 **(In Japanese)**
Sawada Y (2003) Eruption cloud echo observed with JMA's C-band weather radar. Weather Serv Bull 70:119–169 **(In Japanese)**
Suzuki YJ, Koyaguchi T (2015) Effects of wind on entrainment efficiency in volcanic plumes. J Geophys Res Solid Earth 120:6122–6140. https://doi.org/10.1002/2015JB012208
Terada A (2018) Kusatsu-Shirane volcano as a site of phreatic eruptions. Jour Geol Soc Japan 124:251–270. https://doi.org/10.5575/geosoc.2017.0060 (**In Japanese with English abstract**)
Tseng KH, Ogawa Y, Nurhasan TSB, Ujihara N, Honkura Y, Terada A, Usui Y, Kanda W (2020) Anatomy of active volcanic edifice at the Kusatsu-Shirane volcano, Japan, by magnetotellurics: hydrothermal implications for volcanic unrests. Earth Planets Space 72:161. https://doi.org/10.1186/s40623-020-01283-2
Woodhouse MJ, Hogg AJ, Phillips JC (2016) A global sensitivity analysis of the PlumeRise model of volcanic plumes. J Volcanol Geotherm Res 326:54–76. https://doi.org/10.1016/j.jvolgeores.2016.02.019
Woodhouse MJ, Hogg AJ, Phillips JC, Sparks RSJ (2013) Interaction between volcanic plumes and wind during the 2010 Eyjafjallajokull eruption, Iceland. J Geophys Res Solid Earth 118:92–109. https://doi.org/10.1029/2012JB009592
Yaguchi M, Ohba T, Numanami N, Kawaguchi R (2019) Constituent mineral and water-soluble components of volcanic ash from the 2018 eruption of Mt. Motoshirane of Kusatsu-Shirane Volcano, Japan. J Disaster Res 14:991–995. https://doi.org/10.20965/jdr.2019.p0991
Yamada T, Kurokawa AK, Terada A, Kanda W, Ueda H, Aoyama H, Ohkura T, Ogawa Y, Tanada T (2021) Locating hydrothermal fluid injection of the 2018 phreatic eruption at Kusatsu-Shirane volcano with volcanic tremor amplitude. Earth Planets Space 73:14. https://doi.org/10.1186/s40623-020-01349-1

Publisher's Note